Tribology International 48 (2012) 15–21

Contents lists available at ScienceDirect

Tribology International

journal homepage: www.elsevier.com/locate/triboint

An experimental study on the relation between surface texture and tactile friction

J. van Kuilenburg [a,b,*], M.A. Masen [b], M.N.W. Groenendijk [c], V. Bana [d], E. van der Heide [a,b]

[a] TNO Science and Industry, PO Box 6235, 5600 HE Eindhoven, The Netherlands
[b] University of Twente, Faculty of Engineering Technology, PO Box 217, 7500 AE Enschede, The Netherlands
[c] Lightmotif BV, Pantheon 12, 7521 PR Enschede, The Netherlands
[d] Philips Consumer Lifestyle, Tussendiepen 4, 9200 CA Drachten, The Netherlands

ARTICLE INFO

Article history:
Received 1 October 2010
Received in revised form
13 April 2011
Accepted 1 June 2011
Available online 16 June 2011

Keywords:
Skin friction
Touch
Surface texture
Laser texturing

ABSTRACT

The main obstacle to calculate the 'feel' of a product from its surface properties is the ill-defined surface topography that is encountered after the most surface finishing processes. In this work this obstacle was avoided by producing well-defined surface topographies by laser texturing. The friction of textures having surface features with varying radii and spacings was investigated by measuring friction against the fingerpad. Within the range of conditions tested the coefficient of friction decreased with increasing normal load. The relation between the surface texture parameters and the coefficient of friction is influenced by the scale-dependent elastic behaviour of the skin top layer.

1. Introduction

The finishing of the surface of a product determines to a large extent its 'look and feel'. During touch, surface features in contact with the skin cause a load distribution at the skin surface and thereby a stress and strain distribution within the skin. The load distribution at the skin surface is altered by the frictional behaviour when sliding between the skin and the product surface occurs. Stresses and strains at mechanoreceptor locations within the skin evoke responses of the receptors, which are sent to the brain through the nerves. The activity of the central nervous system then produces a sensation, which can be quantified in terms of perceived magnitude: the descriptive level. Finally, a value judgement of the sensation, a perceived quality of feel can be made: the emotional level. Optimisation of product surface tactile properties is frequently achieved through trial and error. The development of guidelines, which will enable industry to predict and optimise the emotional qualities and expectations associated with specific surface finishes has recently become the subject of tribological research, see e.g. [1,2,3].

The main obstacle to calculate the 'feel' of a product from the surface properties and geometry is the ill-defined surface topography that is encountered after the most surface finishing processes such as grinding or blasting. The complicated scale dependence of roughness makes it difficult to pinpoint the feel to a certain geometric parameter [1]. This obstacle can be avoided by producing well-defined surface topographies [2]. In this work well-defined surface textures consisting of evenly distributed small scale surface bumps were produced by laser texturing. The ability of this technique to produce well-defined surface features has already been used to produce micro-dimples acting as micro-hydrodynamic bearings or micro-reservoirs in lubricated contacts. In dry contacts these micro-dimples might trap wear particles, thus reducing friction and wear [4].

Understanding product feel and comfort of product surfaces, packaging material or medical textiles begins with an understanding of the frictional behaviour [4–6]. Analytical expressions for describing the friction against human skin have been thoroughly described by Adams et al. [7] and are used in this work for comparison with the frictional behaviour observed in experiments on these textured surfaces. The well-defined texture will make it possible to calculate the feel from the surface topography, starting with the prediction of the coefficient of friction.

2. Experimental

When assuming elastic behaviour of the skin several expressions describing the frictional behaviour are available from literature [7]. Since in the contact with a random rough surface adhesion is the

* Corresponding author at: University of Twente, Faculty of Engineering Technology, PO Box 217, 7500 AE Enschede, The Netherlands. Tel.: +31 6 508 66 246.
E-mail addresses: j.vankuilenburg@utwente.nl, julienvk@hotmail.com (J. van Kuilenburg).

0301-679X/$ - see front matter © 2011 Elsevier Ltd. All rights reserved.
doi:10.1016/j.triboint.2011.06.003

dominant friction mechanism, the coefficient of friction is determined by the magnitude of the real contact area. Following for example Greenwood and Williamson theory for the contact of random rough surfaces the coefficient of friction can be expressed as a function of roughness amplitude and mean asperity radius. These roughness parameters amplitude and asperity radius are mean values taken from a set of measured amplitudes and radii. Furthermore, these roughness amplitudes and radii depend strongly on measuring equipment and method. Using regular surface textures these uncertainties are avoided and the coefficient of friction can be predicted with greater accuracy.

2.1. Materials

Four different surface structures were made with picosecond laser pulses. Metal samples were produced directly on stainless strip material using laser ablation [8]. Polymer samples were produced by applying the structures on mould inserts and reproduction in a thermoplastic polyurethane (TPU). The macro-geometry of the samples is a circular flat with a 30 mm diameter. Micro-geometrical parameters of the different surface textures are summarised in Table 1.

The surface texture is composed from bumps having a spherical tip with radius R, which are evenly distributed with a spacing λ between the tips as depicted in Fig. 1. Four different surface textures were composed from two different radii and two different spacings. Radii and spacings were chosen such that the minimum and maximum values of the radius over spacing R/λ differ by one order of magnitude, while the tip radii are small. A small tip radius was expected to result in a low contact area and thus relatively low friction.

SEM images of the metal and TPU samples are shown in Figs. 2 and 3, respectively. Fig. 2 is representative for all metal samples and the injection moulded textures with tip radii $R=5$ μm. The two-dimensional waved surface described by a spacing and tip radius approaches a bi-sinusoidal surface with its crests, valleys and saddle points. With the injected moulded textures with tip radii $R=1$ μm the saddle points are stretched appearing as ridges surrounding relatively large square valleys with the crests as small scale surface features superposed on this grated pattern as can be seen from Fig. 3. It needs no explanation that the mechanisms responsible for the frictional behaviour of such a grated texture might be completely different than those of the bi-sinusoidal texture of Fig. 2. A further analysis of the contact mechanisms for such grated textures is not considered relevant within the scope of this work.

The metal and TPU samples were tested against the fingerpad skin of the left (dominant) index finger of a 35-year old male subject.

Table 1
Surface textures produced by picosecond laser pulses. All textures are applied on metal and TPU (denoted as m1, m2, etc. and TPU1, TPU2, etc.).

No.	Radius R (μm)	Spacing λ (μm)	R/λ (dimensionless)	Height h (μm)
1	1	30	0.033	30
2	1	60	0.017	30
3	5	60	0.083	20
4	5	30	0.167	20

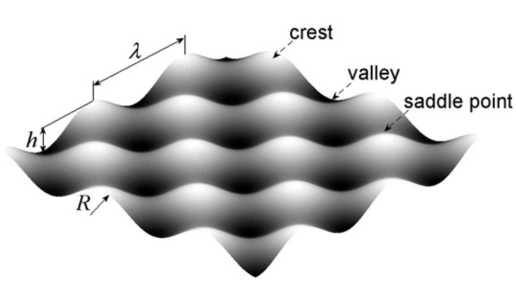

Fig. 1. Definition of texture parameters of test samples produced by laser texturing.

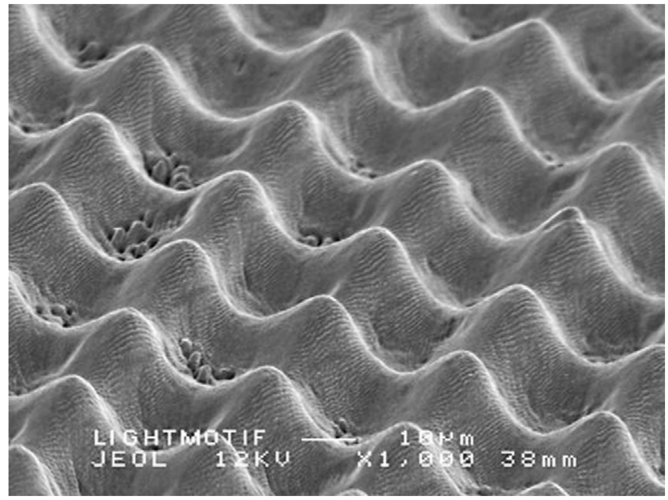

Fig. 2. SEM image of metal sample (m4) with tip radius $R=5$ μm and spacing $\lambda=30$ μm.

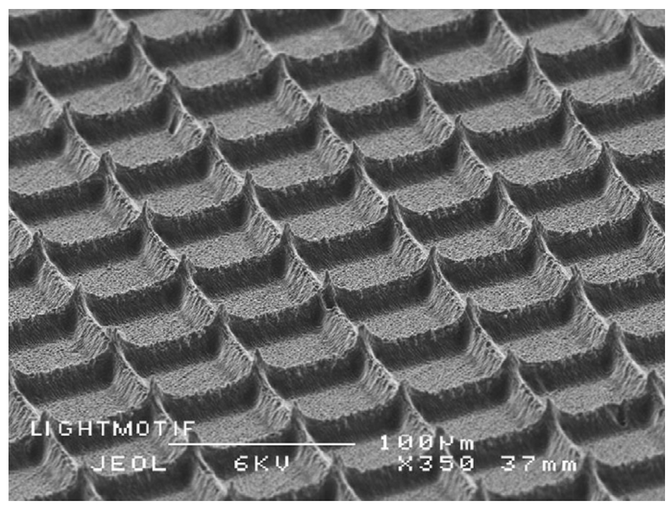

Fig. 3. SEM image of TPU sample (TPU2) with tip radius $R=1$ μm and spacing $\lambda=60$ μm.

2.2. Methods

Sliding friction was measured in vivo against human skin using the Skin Micro-Tribometer model UMT (CETR, USA) described by e.g. Sivamani et al. [9]. The tribometer was equiped with a 6-axis torque /force sensor (type TFH-6), which measures normal load in the range 0.5–60 N (7.5 mN resolution) and lateral (friction) loads in the range 0.2–20 N (2.5 mN resolution). The normal loads used were 0.5, 1 and 2 N. Stroke distance in fingerpad measurements was 12 mm at a sliding velocity of 12 mm/s. For the measurements of friction of the fingerpad the left index finger of the experimenter was positioned on a support under the sliding probe at an inclination of about 30°.

All tests were carried out at the room temperature of 20 ± 2 C° and relative humidity 45 ± 4%. Each measurement consists of

3 cycles back-and-forth. The mean of the 6 strokes was taken as the mean coefficient of friction μ.

During the test programme the hydration level of the fingerpad skin surface was determined using a Corneometer® CM 825 (CK electronic GmbH, Germany). This device measures the hydration level of the upper 10–20 μm of the stratum corneum through capacitance. The hydration level is expressed in arbitrary units, AU, <30 AU corresponding to dry skin, >50 AU corresponding to hydrated skin. The strong correlation between skin hydration level measured using the Corneometer® CM 825 and skin friction is illustrated by Gerhardt et al. [10].

2.3. Sample preparation

All samples were cleaned using ethanol before and in between the experiments. Before carrying out the experiments, the hands were washed using water and soap and air dried. After a rest period of approximately 10 min to allow the washed skin to regain its normal condition the experiments on dry skin were carried out. Experiments on hydrated skin were carried out after submersion in water for at least 10 min. The fingerpad skin was hydrated by submersion, the skin of the forearm was hydrated using a wet sponge. Verrillo et al. [11] showed that after submersion from 5 to 10 min hydration returns to normal levels between 5 and 15 min, much longer than the time needed for one experiment. Before the experiments excess water was removed using a paper tissue.

3. Results and discussion

An overview of the coefficients of friction measured against dry skin is shown in Fig. 4. The mean coefficient of friction is given for the metal (m) and TPU samples for different normal loads. Smooth, non-textured samples were measured for reference and are noted as m0 and TPU0.

3.1. General discussion

The development of the contact area of a fingertip and a smooth surface was investigated by several authors [2,12]. Soneda and Nakano [12] measured the apparent and real contact areas of fingerpads as a function of contact load. For normal loads between 0.1 and 5 N they found the real contact area to increase with contact load following a power law with exponent 0.68. They defined the real contact area as the area of the fingerprint ridges in contact with the smooth, flat surface and the apparent contact area as the area within the outline of the real contact area. In this work the apparent, or nominal, contact area A_0 is defined as the area of the fingerprint ridges in macroscopic contact with the countersurface. The real contact area A_r is defined as the total area of the surface features, which are in actual contact with the skin.

3.1.1. Friction of regular surface textures

The coefficient of friction is composed of a deformation and an adhesion component

$$\mu = \mu_{def} + \mu_{adh} \tag{1}$$

Expressions for the deformation and adhesion components of friction for a spherical indenter sliding against the skin are discussed by e.g. Adams et al. [7] and can be rewritten for the textures produced in this study. Since the surface features are arranged in a regular pattern having a pillar spacing λ, the number of surface features N in contact with the skin can be approximated from the contact area A_0 using

$$A_0 = N\lambda^2 \tag{2}$$

The total normal load F_n is composed of the normal loads on each surface feature $F_{n,i}$ following:

$$F_n = NF_{n,i} \tag{3}$$

Assuming that the individual surface features of the textures are perfectly spherical and assuming elastic behaviour of the skin, the equations adopted from [6] can be rewritten by substituting Eqs. (2) and (3).

The coefficent of friction for deformation can now be expressed as a function of normal force F_n, real contact area A_0 and a surface texture parameter R/λ, the quotient of surface feature radius and spacing, following:

$$\mu_{def} \propto \beta E^{*(-1/3)} \left(\frac{R}{\lambda}\right)^{-2/3} \left(\frac{A_0}{F_n}\right)^{-1/3} \tag{4}$$

where E^* is the effective elastic modulus, in case of a countersurface having a high elastic modulus determined mainly by the skin elastic modulus and β the skin viscoelastic loss fraction. This viscoelastic loss fraction can be estimated from the hysteresis

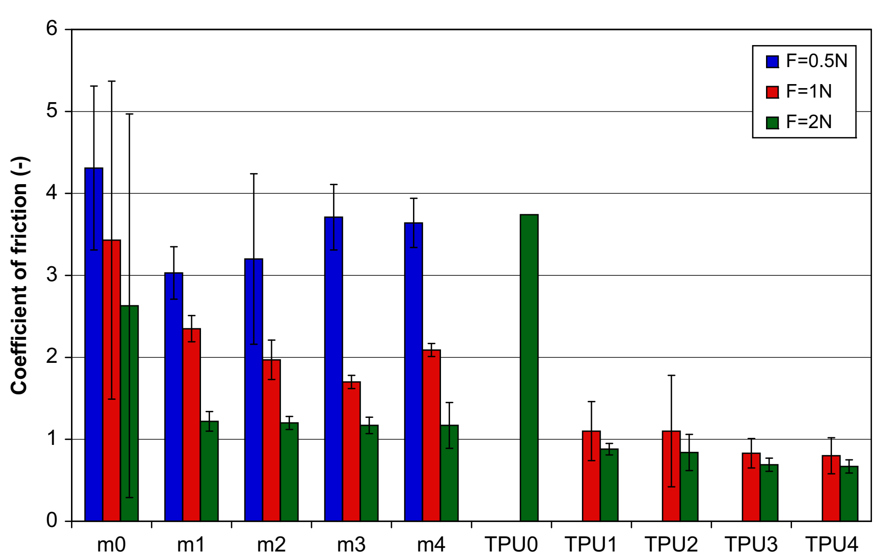

Fig. 4. Overview of the coefficients of friction (mean ± 2 st. dev.) measured for metal (m) and TPU samples, m0 and TPU0 being smooth reference samples.

loop, the area between the loading and unloading curve in an indentation experiment.

The coefficient of friction for adhesion can be expressed as

$$\mu_{adh} \propto \tau E^{*(-2/3)} \left(\frac{R}{\lambda}\right)^{2/3} \left(\frac{A_0}{F_n}\right)^{1/3} \tag{5}$$

where τ is the shear stress of the skin-texture interface thus giving the friction force due to adhesion when being multiplied with the total area of the surface features in contact with the skin. The total coefficient of friction for the textures produced in this study can be expressed as a function of surface texture parameter R/λ by substituting Eqs. (4) and (5) into (1):

$$\mu_{text} \propto C_{def} \left(\frac{R}{\lambda}\right)^{-2/3} + C_{adh} \left(\frac{R}{\lambda}\right)^{2/3} \tag{6}$$

Values for contact area of the fingerpad as a function of normal load are measured by e.g. Childs et al. [2] and Soneda and Nakano [12]. At normal loads around $F_n = 2$ N, the contact area A_0 varies from 30 to 60 mm^2. For A_0 a value of 60 mm^2 is adopted. Mechanical properties from dry stratum corneum can be found in literature $\beta \sim 0.31$, $E_{sc} \sim 100$ MPa [13] and $\tau \sim 10$ MPa [14]. Using these values the parameters C_{def} and C_{adh} can be calculated. It is found that $C_{adh} \sim 1.4$, thus being much larger than $C_{def} \sim 0.02$. From this it is expected that adhesion is the dominant mechanism within the range of texture parameters investigated in this work.

3.1.2. Elastic behaviour of the contact zone

The validity of Eqs. (4) and (5) is based on the assumption of elastic behaviour of the contact zone. Furthermore, it is assumed that the real contact area is determined mainly through the properties of the stratum corneum, having a high stiffness, as opposed to the much more compliant epidermis. For this assumption to be valid, the contact radius of each individual surface feature, the Hertzian contact radius, a should be smaller than the radius of this surface feature:

$$a = \left(\frac{3F_{n,i}R}{4E^*}\right)^{1/3} < R \tag{7}$$

Expressing the normal force on the contact in texture parameters R and λ using Eqs. (2) and (3) and setting the contact radius equal to the tip radius yields the following expression for the minimum elasticity for the above assumption to be valid:

$$E^* > \frac{3}{4}\left(\frac{R}{\lambda}\right)^{-2} \frac{F_n}{A_0} \tag{8}$$

When adopting the same values for normal load and nominal contact area as in Section 3.1.1 (2 N and 60 mm^2, respectively), for $R/\lambda = 0.017$, the smallest value of all samples used in the present study, an equivalent elastic modulus of the skin is required that exceeds 86 MPa. Pailler-Mattei et al. [15] and Yuan and Verma [13] report values for the stratum corneum elastic modulus obtained from indentation measurements, which for dry skin exceed the value of 86 MPa. From this it may be concluded that the assumption of elastic behaviour at the scale of the surface features is valid.

3.2. Friction of metal samples

The coefficient of friction measured of metal samples against the fingerpad is plotted as a function of normal load in Fig. 5. The frictional behaviour of a smooth, non-textured, metal sample was measured for reference.

Since we know from e.g. Adams et al. [7] and the theory in Section 3.1 that adhesion is the dominant mechanism in the majority of contacts involving human skin, from Eq. (5) a clear relation between the coefficient of friction and R/λ is expected. The theory of adhesion being the dominant mechanism is supported by the dependence of the coefficient of friction on the normal load, as shown in Fig. 5. For the smooth surface the coefficient of friction decreases with normal load following a power law with power −0.36. Assuming that adhesion is the dominant friction mechanism the measured friction force is directly proportional to the real contact area, so that the coefficient of friction is given by

$$\mu = \frac{\tau A_r}{F_N} \tag{9}$$

where the real contact area A_r is known to depend on the normal load following:

$$A_r \propto F_N^a \tag{10}$$

The coefficient of friction between the skin of the fingerpad and a smooth surface is thus expected to depend on the normal load as

$$\mu \propto F_N^{\,a-1} \tag{11}$$

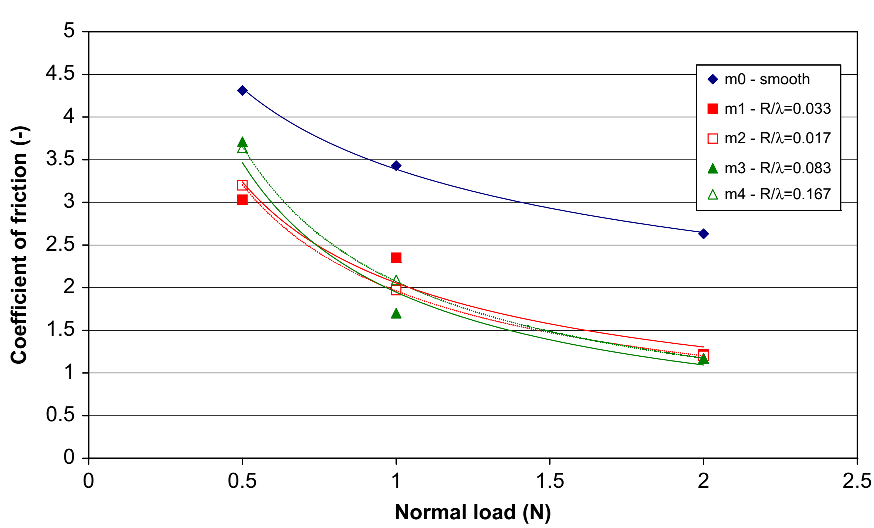

Fig. 5. Coefficient of friction as a function of normal load for metal samples.

From the experimental results for F_N an exponent $a-1=-0.36$ was measured, so in Eq. (10) $a=0.64$. This value corresponds well with the exponent 0.68 ± 0.09 found by Soneda and Nakano [12] for normal loads between 0.1 and 5 N.

A non-linear decrease of the coefficient of friction with normal load is observed for random roughness as well [5,16,17]. The coefficient of friction of the textured surfaces is related with normal force through a power law with the power n ranging from -0.83 to -0.65, which is much stronger than we would expect from Eq. (5). From Eqs. (5) and (10), which describe the relation between contact area and normal load, the coefficient of friction is expected to depend on the normal load following:

$$\mu \propto \left(\frac{A_0}{F_N}\right)^{1/3} \propto F_N^{1/3(a-1)} \tag{12}$$

Since the contact area increases with normal load the exponent in Eq. (10) $a>0$, so according to Eq. (12) the coefficient of friction of the textured surfaces will depend on the normal load with an exponent $n>-1/3$. However, an exponent n ranging from -0.83 to -0.65 was measured. The strong dependence of the measured coefficient of friction on the applied normal load is expected to be caused by normal adhesion, which increases the effective normal load on the contact spots. The measured friction load $F_{\mu,meas}$ is related to the applied normal load F_N through the measured coefficient of friction μ_{meas}

$$F_{\mu,meas} = \mu_{meas} F_N \tag{13}$$

The measured friction load can also be expressed as the product of the coefficient of friction μ and the effective normal load at the contact area which is composed of the applied normal load F_N and the load due to normal adhesion F_{adh}:

$$F_{\mu,meas} = \mu(F_N + F_{adh}) \tag{14}$$

The measured coefficient of friction thus depends on the applied normal load following:

$$\mu_{meas} = \frac{F_{\mu,meas}}{F_N} = \mu\left(1+\frac{F_{adh}}{F_N}\right) \tag{15}$$

which expression also shows that the relative contribution of adhesion decreases with increasing normal load.

Fig. 6 shows the coefficient of friction as a function of texture parameter R/λ. For the surface texture parameter R/λ no relation with the coefficient of friction can be determined from Fig. 6. From Eq. (5) the coefficient of friction would be expected to increase with increasing parameter R/λ. However, up to this point the equivalent elastic modulus is assumed to have a constant value. From indentation measurements (e.g. Yuan and Verma [13]) a clear lengthscale effect can be observed: the effective elastic modulus decreases with increasing indentation depth at constant indenter radius and decreases with decreasing indenter radius at constant indentation depth. An increase of the surface parameter R/λ thus involves an increase in effective elastic modulus E^*. The total effect of these mechanisms depends on the magnitude of radius, spacing and normal load, but observation of Eq. (5) learns that an increase in both R/λ and E^* conceals a clear effect of the surface texture parameter.

3.3. Friction of TPU samples

Fig. 7 shows the coefficient of friction as a function of normal load. Fig. 8 shows the coefficient of friction as a function of texture parameter R/λ for dry and hydrated skin.

From Figs. 7 and 8 a decrease of the coefficient of friction with surface texture parameter R/λ can be observed for non-hydrated skin. From Fig. 7 it can be seen that this decrease is mainly a dependence on tip radius R. The injection moulded textures with tip radii $R=5$ μm have a two-dimensional waved surface, whereas the textures with tip radii $R=1$ μm have a grated pattern with small scale surface features superposed on this pattern as shown in Fig. 3. The theory proposed in Section 3.1 assumes the contact area being built up from Hertzian contacts at the asperity level, which applies for the two-dimensional waved surface with tip radius $R=5$ μm. For the textures with tip radii $R=1$ μm the grating is in contact with the skin as well, demanding a more complicated contact model as discussed in Section 3.1.1.

Comparison of the mechanisms responsible for the frictional behaviour of these two different sets of textures is therefore considered irrelevant within the scope of this work.

Fig. 8 shows the difference in frictional behaviour between non-hydrated and hydrated skin. The hydration level of non-hydrated skin during the test programme was 70 ± 8 AU, for hydrated skin it was higher 110 ± 6 AU. This increase in hydration level of the skin of the fingerpad corresponds to observations of Verrillo et al. [11], who reported an increase of 35% after submersion in water. This relatively small increase in hydration level as compared to the differences observed at other anatomical sites is due to the relatively high baseline level of the fingerpad. The biological function of this higher level of hydration is to increase the coefficient of friction during manipulating tasks.

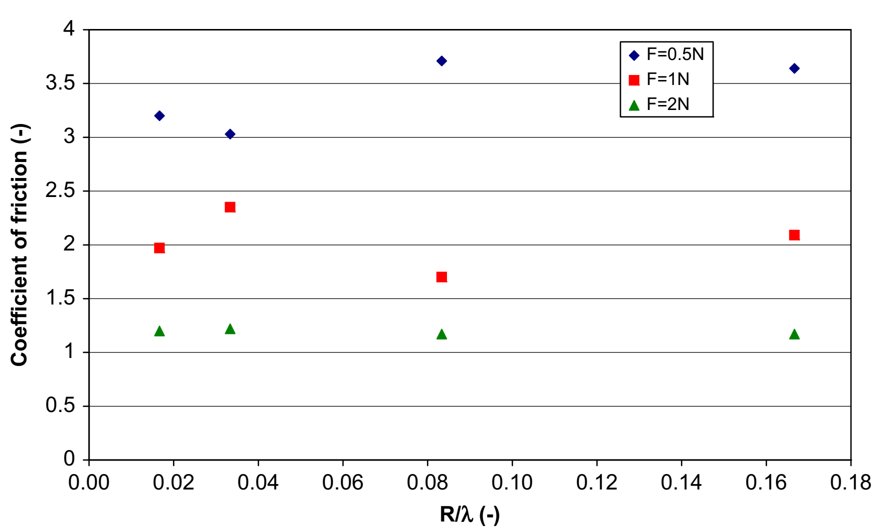

Fig. 6. Coefficient of friction as a function of texture parameter R/λ for metal samples.

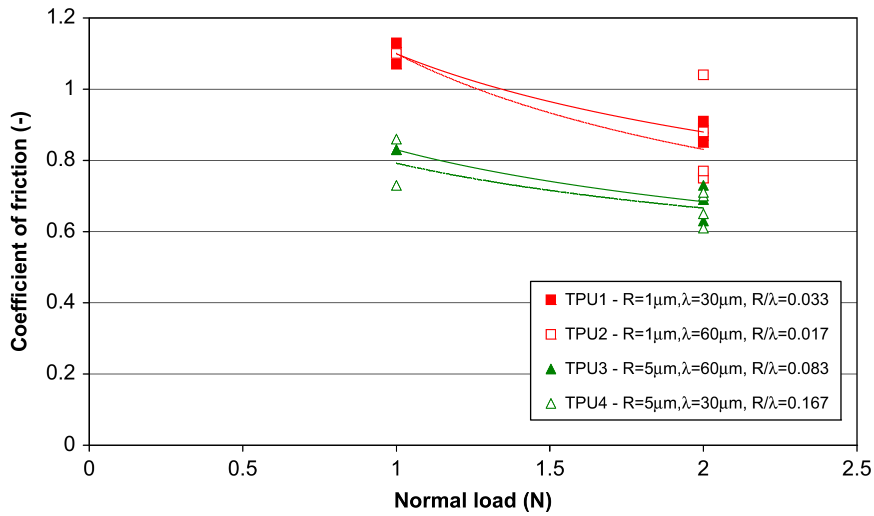

Fig. 7. Coefficient of friction as a function of normal load for TPU samples.

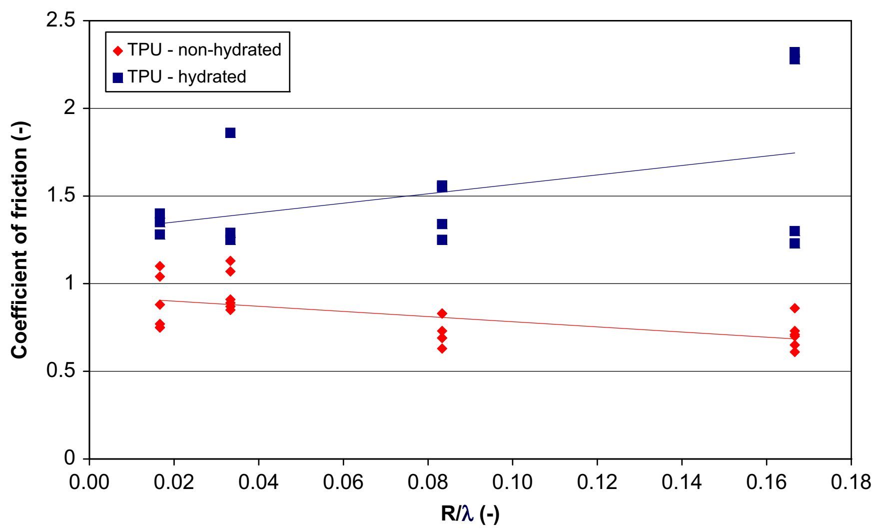

Fig. 8. Coefficient of friction as a function of texture parameter R/λ and for TPU samples sliding against non-hydrated and hydrated skin.

Coefficients of friction for the non-hydrated fingerpad range from 0.6 to 1.1. For the hydrated fingerpad coefficients of friction between 1.25 and 2.3 were measured. The increase in friction with the skin surface hydration level is mainly caused by softening of the stratum corneum. The increase of friction with hydration measured against TPU corresponds to earlier observations by e.g. Derler et al. [5], Sasada [16] and André et al. [17,18].

4. Conclusions

Friction of well-defined regular surface textures produced with picosecond laser pulses was measured against the skin of the fingerpad. The coefficient of friction decreased strongly with normal load for both metal and TPU surfaces supporting the theory that adhesive friction is the dominant friction mechanism. The strong dependence of the measured coefficient of friction on the applied normal load is expected to be caused by normal adhesion, which increases the effective normal load on the contact spots.

Experiments with TPU against hydrated skin showed an increase of the coefficient of friction with a factor two compared to dry skin. Within the range of surface feature geometries investigated no clear relation was found between feature geometry and coefficient of friction. This is probably due to scale-effects of the elastic behaviour of the stratum corneum counteracting with the influence of variation in feature geometry.

Fabrication of surface structures by laser texturing using picosecond laser pulses has proven to be a useful technique for producing well-defined micro-scale surface textures. The control of texture parameters for the injection moulded surfaces needs further work. The frictional behaviour of these micro-scale textures is determined by the properties of the stratum corneum. Considering the stratum corneum has a high elastic modulus optimisation of textures produced by laser texturing is expected to bring forth surfaces having very low friction.

Further work will involve a parameter study to gain more understanding of the relation of surface feature geometry and scale-effects in the elastic behaviour of the stratum corneum. An experimental programme involving a larger number of subjects should give insight in the robustness of the theories describing the frictional behaviour.

Furthermore, this study will be extended to measuring the response of subjects to the different surface textures to provide a basis for calculation of the 'feel' of these surfaces.

Acknowledgements

This research was carried out under the Project number MA.08113 in the framework of the Research Programme of the Materials Innovation Institute M2i (www.m2i.nl).

References

[1] Barnes CJ, Childs THC, Henson B, Southee CH. Surface finish and touch—a case study in a new human factors tribology. Wear 2004;257:740–50.
[2] Childs THC, Henson B. Human tactile perception of screen-printed surfaces: self-report and contact mechanics experiments. Proc IMechE Part J: J Eng Tribol 2007;221:427–41.
[3] Liu X, Yue Z, Cai Z, Chetwynd DG, Smith ST. Quantifying touch-feel perception: tribological aspects. Meas Sci Technol 2008;19:08007-1–9.
[4] Etsion J. State of the art in laser surface texturing. J Tribol Trans ASME 2005;127:248–53.
[5] Derler S, Gerhardt L-C, Lanez A, Bertaux E, Hadad M. Friction of human skin against smooth and rough glass as a function of the contact pressure. Tribol Int 2009;42:1565–74.
[6] Skedung L, Danerlöv K, Olofsson U, Aikala M, Niemi K, Kettle J, Rutland MW. Finger friction measurements on coated and uncoated printing paper. Tribol Lett 2010;37:389–99.
[7] Adams MJ, Briscoe BJ, Johnson SA. Friction and lubrication of human skin. Tribol Lett 2007;263:239–53.
[8] Römer GRBE, Huis in't Veld AJ, Meijer J, Groenendijk MNW. On the formation of laser induced self-organizing nanostructures. CIRP annals—manufacturing technnology, vol. 58; 2009. p. 201–4.
[9] Sivamani RK, Goodman J, Gitis NV, Maibach HI. Friction coefficient of skin in real-time. Skin Res Technol 2003;9:235–9.
[10] Gerhardt L-C, Strässle V, Lenz A, Spencer ND, Derler S. Influence of epidermal hydration on the friction of human skin against textiles. J R Soc Interface 2008;5:1317–28.
[11] Verrillo RT, Bolanowski SJ, Checkosky CM, McGlone FP. Effects of hydration on tactile sensation. Som Mot Res 1998;15:93–108.
[12] Soneda T, Nakano K. Investigation of vibrotactile sensation of human fingerpads by observation of contact zones. Tribol Int 2009;43:210–7.
[13] Yuan Y, Verma R. Measuring microelastic properties of stratum corneum. Coll Surf B: Bioint 2006;48:6–12.
[14] Wu KS, Van Osdol WW, Dauskardt RH. Mechanical properties of human stratum corneum: effects of temperature, hydration, and chemical treatment. Biomat 2006;27:785–95.
[15] Pailler-Mattei C, Pavan S, Vargiolu R, Pirot F, Falson F, Zahouani H. Contribution of stratum corneum in determining bio-tribological properties of the human skin. Wear 2007;263:1038–43.
[16] Sasada T. The friction of human skin. In: Proceedings of 21st biotribological symposium. Fukuoka, Japan; 2000. p. 46–52.
[17] André T, Lefèvre P, Thonnard J-L. A continuous measure of fingertip friction during precision grip. J Neurosci Methods 2009;179:224–9.
[18] André T, De Wan M, Lefèvre P, Thonnard J-L. Moisture elevator: a direct measure of fingertip skin hydration during object manipulation. Skin Res Technol 2008;14:385–9.